J. Helminthol. Soc. Wash.
58(1), 1991, pp. 69–81

Light and Electron Microscopical Study of a Bacterial Parasite from the Cyst Nematode, *Heterodera glycines*

RICHARD M. SAYRE,[1] WILLIAM P. WERGIN,[2] TSUTOMU NISHIZAWA,[3] AND MORTIMER P. STARR[4,5]

[1] Nematology Laboratory, Plant Sciences Institute, Beltsville Agricultural Research Center, USDA, ARS, Beltsville, Maryland 20705,
[2] Electron Microscopy Laboratory, Natural Resources Institute, Beltsville Agricultural Research Center, USDA, ARS, Beltsville, Maryland 20705,
[3] Laboratory of Nematology, National Institute of Agro-Environmental Sciences, Tsukuba, Ibaraki 305, Japan, and
[4] Department of Microbiology, University of California, Davis, California 95616

ABSTRACT: The host range and morphology of a mycelial and endospore-forming bacterium (CNP) that parasitizes the cyst nematode, *Heterodera elachista,* differentiates it from 2 related species, *Pasteuria penetrans* and *Pasteuria thornei,* parasites of *Meloidogyne* spp. and *Pratylenchus* spp., respectively. In cross-inoculation experiments with the 3 bacteria, the CNP parasitized the nematodes *Heterodera glycines* and *Globodera rostochiensis* but not species in either *Meloidogyne* or *Pratylenchus.* The rhomboidal shape of the sporangia of *Pasteuria thornei* distinguishes this species from the other 2 bacteria, which have cup-shaped sporangia. The results of the cross-inoculation studies and differences in the fine structure of the cup-shaped sporangia suggest that CNP should be assigned to a new species within the genus *Pasteuria.*

KEY WORDS: plant-parasitic nematodes, soil bacterium, *Pasteuria* spp., soybeans, morphology, scanning electron microscopy (SEM), transmission electron microscopy (TEM).

A recent revision of the genus *Pasteuria* delineated 2 species, *Pasteuria penetrans* Starr and Sayre, 1988, sensu stricto and *Pasteuria thornei* Starr and Sayre, 1988 (Starr and Sayre, 1988; Sayre and Starr, 1989), which are parasites of the root-knot nematode, *Meloidogyne incognita* (Kofoid and White, 1919) Chitwood, 1949, and the root-lesion nematode, *Pratylenchus brachyurus* (Godfrey, 1929) Filipjev and Schuurmans Stekhoven, 1941, respectively. Recently, another possible member of the genus *Pasteuria* was found by Nishizawa (1984) parasitizing *Heterodera elachista* Oshima, 1974. Following his initial observation, Nishizawa (1986) associated the field presence of the bacterium with a decline in the population of the cyst nematode. Confirmation of this phenomenon was noted at the Tochigi Agricultural Experiment Station where soybean breeding lines were being screened for cyst nematode resistance (Nishizawa, 1987).

The present study uses light and electron microscopy to compare the morphology of this recently discovered bacterium, which parasitizes cyst nematodes with that of *Pasteuria penetrans* and *Pasteuria thornei,* 2 species of bacteria that parasitize some species in the genera *Meloidogyne* and *Pratylenchus,* respectively. Although the nomenclature of the new bacterium will be presented at a later time, in this study the isolate that parasitizes cyst nematodes in the genera *Heterodera* and *Globodera* will be referred to as the "cyst nematode parasite" or CNP.

Materials and Methods

Terminology

The fine structure of the spore wall is used to delineate the species of *Pasteuria* taxonomically. To avoid confusion, in this study we have used the terminology of Sussman and Halvorson (1966) who described *Neurospora* spp., and that of Iterson (1988) who discussed and clarified the terminology of Gram-positive bacteria. Briefly, the following terms will be used: (1) "endospore" refers to the single asexual spore that develops within a sporangium and is surrounded by an exosporium; (2) "endospore wall" is the structure that surrounds the central protoplast or core; (3) "plasma membrane" is the innermost structure that apposes the wall; (4) "cortex" is the multilayered inner spore wall and the outer spore wall; and (5) "perispore" refers to the limiting structures that include the wall layer formed outside the exosporium.

Sources of nematodes

For laboratory bioassays, pure populations of several different species of plant-parasitic nematodes were needed. These populations had the following characteristics: (1) the second stage juveniles (J_2) were healthy, vigorous, and capable of root penetration; (2) the majority of the J_2 were the same physiological age; and

[5] Deceased 29 April 1989.

(3) the juveniles belonged to identified species and races of root-knot or soybean cyst nematodes. Populations with these characteristics were obtained from aseptic cultures of root explants (Lauritis et al., 1982, 1983a, b; Huettel and Rebois, 1985). They consisted of *Meloidogyne incognita, Pratylenchus brachyurus, Heterodera zeae* Koshy, Swarup, and Sethi, 1971, and 4 races of *Heterodera glycines* Ichinohe, 1952. The nematodes were harvested from the cultures using a modified Baermann funnel technique (Niblack and Huang, 1985). In addition to the aseptic cultures, the following nematodes were maintained in greenhouse pot cultures: *M. incognita* on tomato cultivars (cvs.), Marglobe or Tiny Tim; *M. hapla* on a strawberry cv., Sunrise; *M. javanica* on a tomato cv., Marglobe; *H. glycines* on a soybean cv., Kent; *H. zeae* on a corn cv., Iowa Chief; and *P. brachyurus* on a peanut cv., Florarunner. Details for rearing *M. incognita* and *P. brachyurus* were reported previously (Sayre and Wergin, 1977; Sayre et al., 1988). *H. glycines* was maintained in the greenhouse on either soybeans (cv. Kent) or adzuki beans, *Vigna angularis* (Willd.) Ohwi and H. Ohashi (USDA accession 416742). Cysts were extracted from the soil (Ayoub, 1980) and placed on fine-mesh nylon in a Baermann funnel. The hatching J_2 were collected from the funnel over a 2- to 4-day period. Also, examinations of soil samples from previously reported field plot studies of Nishizawa (1987) had isolated 10 additional, commonly occurring, genera or species of plant-parasitic nematodes. These nematodes, which included *Aphelenchoides* sp., *Aphelenchus* sp., *Helicotylenchus* sp., *Globodera rostochiensis, Paratylenchus* sp., *Paratrichodorus porosus, Rotylenchulus reniformis, Tylenchorhynchus* sp., *Tylenchulus semipenetrans,* and *Tylenchus* sp., were also examined for the presence of CNP sporangia on their cuticular surfaces.

Sources of the *Pasteuria* spp.

Methods for the axenic cultivation of *Pasteuria penetrans* have not been reported; however, all isolates of the bacteria were maintained on their respective nematode hosts by the senior author. The cultivation procedure of Stirling and Wachtel (1980) was used to maintain *Pasteuria penetrans* on *M. incognita* infecting tomato plants (cv. Tiny Tim). Tomato roots, which were infested with root-knot nematodes parasitized by *Pasteuria penetrans,* were air-dried and ground into a fine powder. Samples of the powder were rewetted and ground with a pestle and mortar to release the endospores. The bacteria were separated from the plant debris by filtering the suspension through a 500-mesh screen that allowed passage of the sporangia and subsequent collection by centrifugation of the *Pasteuria penetrans* endospores. The source of *Pasteuria thornei* endospores was parasitized J_2 and adults of *P. brachyurus* (Sayre et al., 1988; Starr and Sayre, 1988). The infected nematodes were extracted from the roots of peanut (cf. Florarunner) in a mist chamber (Chapman, 1957). A second source of these endospores was air-dried soil from pots containing peanut roots that were infected with nematodes parasitized by *Pasteuria thornei.* When healthy J_2 and adults of *P. brachyurus* migrated through the contaminated soil, a high proportion of the nematodes were encumbered with endospores of the bacterium.

CNP endospores were obtained from cysts of *H. glycines* that had been imported from Japan (Nishizawa, 1986). To initiate a greenhouse culture in Beltsville, the cysts were crushed in tap water. The number of endospores in this aqueous suspension was measured with a hemocytometer and adjusted to about 1,000 per ml. Juveniles of *H. glycines* (race 3), which were obtained from soybean (cv. Kent) root explant cultures, were suspended in tap water at a concentration of 100 per ml. A 5-ml suspension of J_2 was then filtered through a 47-mm diameter membrane filter (Millipore 0.3-μm pore size). The filter, which retained the J_2, was inverted onto the surface of a 3-ml endospore suspension in a 50-mm diameter Petri dish (Falcon; 1006). The dish was then shaken (50 rpm) for 24–48 hr to allow the endospores to attach to the J_2. The suspension, consisting of the J_2 and their attached endospores, was then pipetted around the roots of soybean seedlings that were grown in 40-mm diameter Cone-Tainers (Ray Leacher Cone-Tainers, Canby, Oregon 97013) containing autoclaved Norfolk loamy sand. Forty-five to 60 days later, the entire plant was removed from the container and the soil was washed from the root system. A dissecting microscope was used to examine the root system for parasitized immature females and mature cysts (Ayoub, 1980). Visual selection and removal of parasitized cysts were difficult because less than 10% of the cysts were diseased. However, the diseased females and cysts were generally smaller, duller, or more opaque than healthy cysts. The opacity resulted from bacterial and/or fungal colonizers of cysts. In addition, the diseased cysts usually sank to the bottom of the sampling dishes while the healthy cysts generally floated on the surface. Finally, the presence of the normal reproductive structures in adult females (i.e., uterus, ovaries, and eggs), or the presence of eggs in cysts, indicated that the bacterial parasite CNP was not present.

Light microscopy of CNP

Cysts parasitized by CNP were crushed and mounted on a microscope slide in a drop of tap water (Southey, 1986). Photomicrographs of CNP were taken with an automatic exposure 35-mm camera attached to a compound microscope (NIKON Microphot F-X) fitted with an interference contrast system. Negatives were obtained on Kodak Tri-X Pan film that was processed in Microdol-X. Morphometric data were obtained by measuring the images in printed enlargements of the photomicrographs.

Previous studies (Sayre and Starr, 1985; Starr and Sayre, 1988) indicated that the measurements of endospores observed by scanning electron microscopy (SEM) were smaller than those obtained by light microscopy. This difference resulted from shrinkage that occurred during fixation, dehydration, and critical-point drying procedures that are required for SEM observation. Consequently, sources of the morphometric data in the present study are designated by the instruments used to obtain the values, e.g., light microscopy data (LM), scanning electron microscopy data (SEM), and transmission electron microscopy data (TEM) (Table 1). All measurements are in micrometers (μm) unless stated otherwise.

Table 1. Comparison of *Pasteuria penetrans, Pasteuria thornei,* and the CNP from cyst nematodes. All measurements are in micrometers.

Characteristic	*Pasteuria penetrans*	*Pasteuria thornei*	CNP
Colony shape	Spherical, to clusters of elongated grapes	Small, elongate clusters	Spherical, to clusters of elongated grapes
Sporangia			
Shape	Cup-shaped	Rhomboidal	Cup-shaped
Diameter			
LM	4.5 ± 0.3	3.5 ± 0.2	5.3 ± 0.3
TEM	3.4 ± 0.2	2.4 ± 0.2	4.4 ± 0.3
Height			
LM	3.6 ± 0.3	3.1 ± 0.2	4.3 ± 0.3
TEM	2.5 ± 0.2	2.2 ± 0.2	3.1 ± 0.3
Episporic structures			
Exosporium	Present, relatively smooth surface	Present, smooth	Present, velutinous to hairy surface
Stem cell	Rarely seen; attachment of a second sporangium sometimes observed	Neither stem cell nor second sporangium seen	Attachment of a second sporangium regularly seen
Central body			
Shape	Oblate spheroid, an ellipsoid sometimes almost spherical, narrowly elliptic in section	Oblate spheroid, an ellipsoid sometimes almost spherical, narrowly elliptic in section	Oblate spheroid, an ellipsoid narrowly elliptic in section
Diameter			
LM	2.1 ± 0.2	1.6 ± 0.1	2.1 ± 0.2
TEM	1.4 ± 0.1	1.3 ± 0.1	1.6 ± 0.2
Height			
LM	1.7 ± 0.2	1.5 ± 0.1	1.7 ± 0.1
TEM	1.1 ± 0.1	1.1 ± 0.2	1.3 ± 0.1
Partial epicortical wall	Surrounds protoplast laterally, not in basal or polar areas	Surrounds protoplast somewhat sublaterally	Entirely surrounds protoplast
Characteristics of pore	Basal annular opening formed from thickened outer wall	Basal cortical wall thins to expose inner central body	Thickness of basal wall constant and is the depth of pore
Pore diameter (TEM)	0.3 ± 0.0	0.1 ± 0.0	0.2 ± 0.0
Episporal structures			
Fibers, origin and orientation	Fibers arise directly from cortical wall, gradually arching downward to form an attachment layer of numerous shorter fibers	Long fibers arise directly from cortical wall, bending sharply downward to form an attachment layer of numerous shorter fibers	Same as *P. penetrans,* but additional layer is formed on the obverse surface of endospore
Matrix, at maturity	Becomes coarsely granular; lysis occurs; sporangial wall collapses; base is vacuolate	Persists, but more granular; some strands are formed and partial collapse may occur	Persists, numerous strands are formed and partial collapse may occur
Host	Root-knot nematodes: *Meloidogyne incognita*	Root-lesion nematodes: *Pratylenchus brachyurus*	Cyst nematodes: *Heterodera* spp., *Globodera rostochiensis*
Completes life cycle in juveniles	No, only in adults	Yes, in all stages	No, only in adults

Scanning electron microscopy of CNP

Nematodes that had been encumbered or parasitized by CNP were chemically fixed, dehydrated, critical point-dried, and coated for SEM observation. The specimens were placed in a 3.0% solution of glutaraldehyde in 0.05 M phosphate buffer (pH 6.8) for at least 1.5 hr, dehydrated in an ethanol series, critical point-dried, and mounted on aluminum stubs. Stubs bearing the dried specimens were sputter coated with 200–300

A of gold-palladium and then examined with a Hitachi S430 or S530 scanning electron microscope operating at 15 or 20 kV. In addition, other specimens were coated with about 30 A of platinum (Wergin and Sayre, 1988; Wergin et al., 1988) and observed in a Hitachi S900 low voltage field emission SEM at 1–2 kV.

Measurements of endospores from SEM micrographs were made either from anaglyphs of digitized images that were collected and viewed with a Kevex 8000 energy dispersive X-ray analyzer equipped with an image-analysis software program, or from stereographic images that were viewed with a 4-mirror stereoscope having a floating light-point attachment. A 10° tilt was used to record the stereo images. The image-analysis program or use of the formula $Z = P/2M \sin(Q/2)$ (where P = parallax value, M = magnification, and Q = tilt angle) was used to obtain the Z measurements (Wergin, 1985).

Transmission electron microscopy (TEM) of CNP

For TEM, single developing females of *H. glycines* parasitized by CNP were hand-picked from soybean roots and placed in a small drop of tap water. The water was mixed with molten 3.0% water-agar at 50°C. After the agar solidified, 0.3–0.5-mm³ blocks of agar, each containing a single diseased individual, were transferred to a vial of 3.0% glutaraldehyde in 0.05 M phosphate buffer (pH 6.8). Following fixation for 3 hr, the specimens were washed in several changes of fresh buffer, postfixed in 2.0% osmium tetroxide for 2 hr, and dehydrated in an acetone series. Finally, the agar blocks were infiltrated with a low-viscosity resin (Spurr, 1969). Silver-gray sections of selected nematodes were cut on a Sorvall MT2 ultramicrotome with a diamond knife and then mounted on uncoated copper grids (75 by 100 mesh). The sections were stained for 10 min with 2.0% aqueous uranyl acetate and then for 5 min with 3.0% lead citrate. The stained thin sections were viewed with a Hitachi H500 transmission electron microscope operating at 75 kV with a 30-μm aperture.

Micrographs of the CNP were compared to those of *Pasteuria penetrans* and *Pasteuria thornei,* which had been prepared by the same procedures as described in earlier studies (Sayre et al., 1983; Sayre and Starr, 1985; Sayre et al., 1988; Starr and Sayre, 1988).

Host specificity

Host specificity was determined by the attachment of bacterial endospores to the cuticles of the J_2 species indicated in Table 2. The J_2 from cultures were counted in a Hawksley chamber, adjusted to 300 per ml, and added to the endospore suspension in a 50-mm Petri dish. To prepare suspensions of the infective endospores of CNP, diseased cysts were hand-picked from the roots of soybean and crushed in 5 ml of water to liberate the sporangia. The resulting suspension was filtered through a 500-mesh wire sieve to remove cuticular debris. The number of sporangia in the suspension was adjusted with a hemocytometer to 5×10^5 per ml. Finally, 5-ml portions of the suspension were added to equal volumes of tap water containing 1,000 J_2.

A shallow pan containing the J_2 and spores was placed on a rotary shaker (50 rpm) and aerated for 24–48 hr. Then, the J_2 were examined with a Leitz inverted microscope at 250× to determine whether endospores had attached to the cuticles of the J_2. When 3–10 endospores had attached to 10% or more of the J_2, the larvae were pipetted around the roots of host plants to determine whether the bacterium would complete its life cycle on a particular nematode host. After 45 days, the seedlings were harvested and their roots were examined for diseased nematode cysts.

Results

Light microscopy

The original Japanese isolate of CNP, which was initially found parasitizing *H. elachista,* was used in all experiments. This Japanese isolate also parasitized 2 additional hosts: *G. rostochiensis* and *H. glycines,* which were reinfected with CNP to maintain a source of the bacterium. Crushing diseased cysts of the soybean nematode, *H. glycines,* in tap water on microscope slides released various stages of the life cycle of CNP, which could be examined and photographed (Fig. 1). LM measurements of the developing bacterium (i.e., immature through mature sporangia) were made from positive photographic prints and compared to those obtained from the 2 other species in the genus *Pasteuria* (Table 1). Generally, 25 separate measurements were taken of a particular stage, and are presented as the mean plus or minus the standard deviation. The mature sporangia exhibited the most distinguishing characteristics of the bacterial isolates; therefore, their features were measured and described (Table 1).

Sporangia were usually found in the opaque cysts (Fig. 2). The mean number of mature sporangia extracted per female was 4.4×10^5. The highly refractile central spore body was oblate spheroid, with axes of 2.1 ± 0.2 by 1.7 ± 0.1. The enveloping lenticular-shaped endospores, which were found attached to the J_2 of *H. glycines* (Fig. 3), measured 5.3 in diameter. Their height, from the margin of the dome of the central body to the base of the sporangium, was 4.0 (Fig. 2). The early, but less frequently found, quartet stage of a developing sporangium had a diameter of 1.8 and measured 3.2 in height from the point of attachment to its distal end (Fig. 4). Similarly, the more mature quartets (Fig. 5) measured 3.0 in diameter and were 3.5 high. In the doublet configuration, the individual sporangium had a diameter of 4.1 and a height of 3.9.

Scanning electron microscopy

Two types of scanning electron microscopes (SEM), a conventional SEM and a low-voltage

field-emission (LVFE) SEM, were used in this study. The LVFE SEM has a resolution approximately 10 times greater than the conventional SEM (Wergin et al., 1988). Mature endospores of CNP, including their associated perisporic remnants and episporal structures, were found adhered to the surfaces of J_2 (Figs. 6, 7) and also to the adult males of *H. glycines* (Figs. 8, 9). The endospores measured about 4.2 in diameter. Two distinct forms of endospores have been observed for CNP (Figs. 6, 7); this observation is similar to that existing in *P. penetrans*. In 1 form, the surface of the endospore is covered by perisporic walls; in the other, the episporic wall structure is exposed. In CNP, the surface appears to be covered by a velutinous membrane, the exosporium. This membrane may be the remnants of the sporangium that had encompassed the surface of the endospore but was not sloughed (Figs. 6, 7). When this material is shed, the exposed surface can be resolved into 2 distinct components: a central body, averaging 1.5 in diameter and 1.2 in height, and a surrounding episporic matrix composed of fine fibers (Fig. 7). In *P. penetrans*, the central body and the related structures measured about 3.3 in diameter and 2.3 in height. Wrinkled perisporic walls covered the *P. penetrans* endospores. The central body in *P. penetrans* was 1.3 in diameter and 1.0 in height; the episporic fibers measured approximately 1.0 in width.

Table 2. Host specificity of RKP (the *Pasteuria* species from root-knot nematodes) and CNP (the cyst nematode parasite from cyst nematodes) as scored by attachments of endospores to nematode J_2.

Nematode	Stage*	*Meloidogyne*-isolate (RKP)	*Heterodera*-isolate (CNP)
Aphelenchoides sp.	J & A	–	–
Aphelenchus sp.	J & A	–	–
Helicotylenchus sp.	J & A	–	–
Heterodera elachista	J_2	–	+
H. glycines	J_2	–	+
H. zeae	J_2	–	–
Globodera rostochiensis	J_2	–	+
Meloidogyne hapla	J_2	+	–
M. incognita	J_2	+	–
M. javanica	J_2	+	–
Paratylenchus sp.	J & A	–	–
Paratrichodorus porosus	J & A	–	–
Pratylenchus brachyurus	J & A	–	–
P. coffeae	J & A	–	–
P. penetrans	J & A	–	–
P. vulnus	J & A	–	–
Rotylenchulus reniformis	J & A	–	–
Tylenchorhynchus sp.	J & A	–	–
Tylenchulus semipenetrans	J & A	–	–
Tylenchus sp.	J & A	–	–

* J, Juveniles; J_2, juveniles, second stage; A, adults.

Transmission electron microscopy of CNP—vegetative growth

The developmental stages (vegetative mycelium, early and late stages of endospore formation, and mature sporangia) of CNP may occur simultaneously in the infected soybean nematode host (Fig. 10). The dichotomously branching hyphal colonies of CNP were septate; the hyphae were bounded by a compound wall, about 0.04 thick, that had outer and inner membranes (Fig. 11). The inner membrane, which opposed the septa, delineated individual cells. Mesosomes were frequently found associated with septa during the vegetative growth (Fig. 11).

Transmission electron microscopy of CNP—endospore formation

In CNP, the sporulation process involved the terminal cells of the microcolonies. These ter-

→

Figures 1–5. Light photomicrographs of the cyst nematode parasite (CNP) from the soybean cyst nematode, *Heterodera glycines*. 1. Numerous sporangia of the CNP released from a crushed cyst. 2. Sporangia of CNP showing their highly refractile central bodies. 3. A juvenile of *H. glycines* with several attached endospores of the CNP. 4. Quartets of early vegetative sporangia. 5. Quartets of late vegetative sporangia that are undergoing endosporogenesis.

Figures 6–9. Scanning electron micrographs of endospores of the cyst nematode parasite (CNP) that are attached to *Heterodera glycines*. 6. CNP endospore attached to a nematode juvenile. The velutinous exosporium covers the central body and its surrounding peripheral fibers. 7. CNP endospore attached to a juvenile of *H. glycines*. The endospore has lost its exosporium revealing the central endosporal body and the surrounding peripheral fibers. 8. CNP endospore attached near the extended copulatory spicules of a male nematode of *H. glycines*. 9. CNP endospore attached to the anterior of an adult male nematode. The endospore blocks the amphidial opening near the slightly protruding stylet.

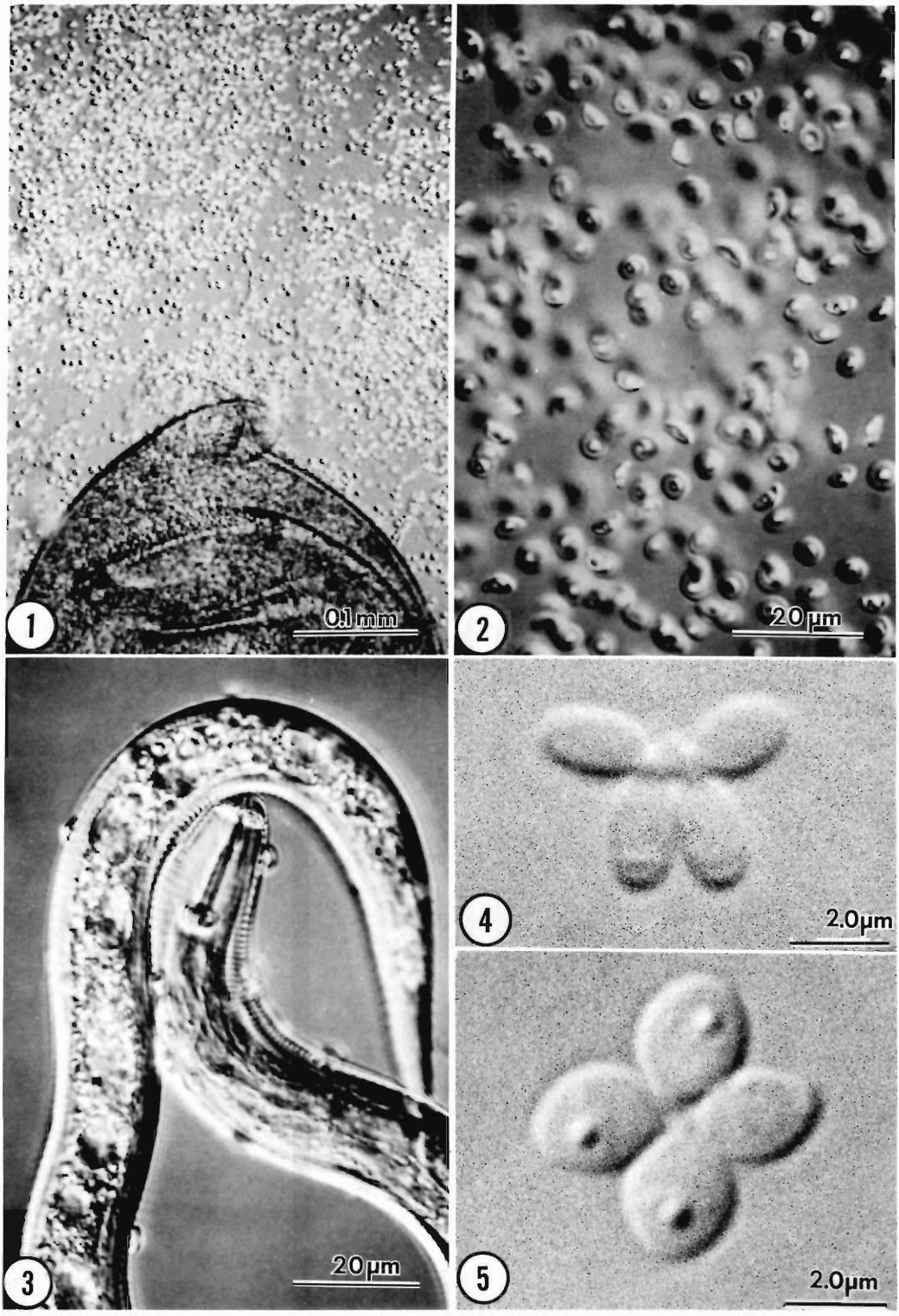

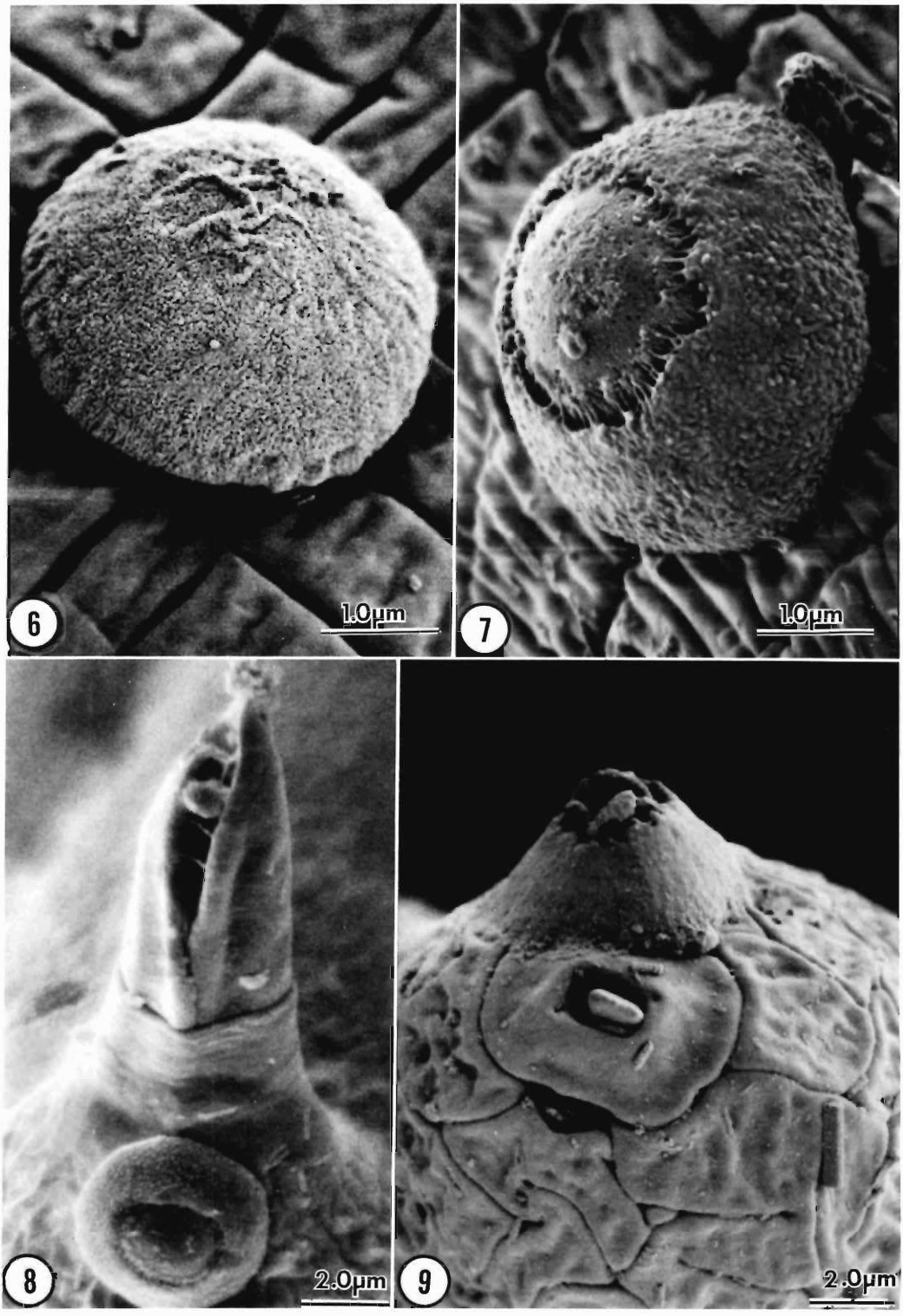

minal cells enlarged and became more ovate (Fig. 12). The protoplasts of the ovate cells, which initially consisted of a granular matrix of ribosomes, gradually exhibited well-defined organelles. During this early transformation, transverse membranes formed within the developing sporangia (Fig. 12). These membranes separated one-third of the upper/distal end of the sporangium, or the developing forespore, from the lower/basal perisporic portion (Fig. 13).

In the later stages of CNP endosporogenesis, the upper end condensed into an electron-dense central core that became encircled by the multilayered wall (Fig. 14). The electron-translucent peripheral region developed laterally with respect to the central body; in later stages, the fibers emerged within these lateral structures, the multilayered walls of the endospore thickened (Fig. 14), and the central body of the endospore became more ellipsoidal. Because the basal matrix of *P. thornei* does not degrade, its sporangium retains a rhomboidal shape at maturity when observed in cross section (Fig. 17).

Transmission electron microscopy of CNP—mature sporangia

In the basal peripheral region of the CNP sporangia, differentiated fibrous strands intermingled with electron-dense granules. Subsequently, the CNP sporangia retained a somewhat lenticular shape in lateral views (Fig. 15). This shape persisted until the outer sporangial wall degraded, thereby exposing the velutinous exosporium (Fig. 6). As a result, the endospore with its accompanying fibers becomes crescent-shaped (Fig. 16) and similar in appearance to the endospores of *P. penetrans.* The mature central body of the CNP endospore is broadly elliptical with axes measuring 1.6 ± 0.2 by 1.3 ± 0.1. One difference between CNP and the other 2 species is the occurrence in the former of an electron-opaque granular layer, or epicortical wall, that surrounds the cortical layer except for an interruption at the basal pore. This structure is not present in the basal or polar areas in *P. penetrans,* and only occurred in the sublateral areas of *P. thornei* en-

→

Figures 10–12. Transmission electron micrographs of the cyst nematode parasite (CNP) from the cyst of the soybean cyst nematode, *Heterodera glycines.* 10. Mycelial colonies (MC) and sporangial stages of the CNP extruded from a cyst of *H. glycines.* Note the simultaneous occurrence of all life stages of the bacterium in this nematode. 11. A portion of a mycelial colony showing early vegetative stages of the CNP. The hyphal walls, which are septate, appear to bifurcate at the margins of the colony. Mesosomes are associated with the septa. 12. An early sporangial stage of the CNP extruded from a cyst of *H. glycines.* A septum delineates the apical forespore of the sporangium from the basal parasporal cell. The compound cell wall of the developing sporangium is composed of an outer and inner membrane.

Figures 13–15. Transmission electron micrographs of the cyst nematode parasite (CNP) from the soybean cyst nematode, *Heterodera glycines.* 13. An electron-opaque body has formed within the forespore. Surrounding the spherical body is a membrane that will condense and contribute to the multilayered wall of the mature endospore. Note the 2 lateral electron-translucent areas that will develop into peripheral fibers. Lysis of cells between the sporangium and the rest of the microcolony allows separation. 14. A sporangium with nearly mature endospore. This endospore, whose multilayered wall has formed, has discernable peripheral fibers. 15. A cross section of a mature sporangium from *H. glycines.* This section shows final stages in differentiation of the endospore that include the formation of an encircling membrane or exosporium and the emergence of the peripheral fibers. Granular material fills the basal portion of the sporangium. The sporangium retains a somewhat lenticular shape in lateral view until the old sporangial wall is fully degraded.

Figures 16, 17. Transmission electron micrographs comparing the endospores of the cyst nematode parasite (CNP) and *Pasteuria thornei.* 16. Cross section of an endospore of the CNP in which the sporangial wall has completely degraded leaving the central body and peripheral fibers surrounded by the velutinous exosporium (EX) and a partial hirsute layer (HC), which have separated from the attachment layers (AL). 17. Cross section of a mature sporangium of *P. thornei,* found parasitizing *Pratylenchus brachyurus,* a root-lesion nematode. The central body of the endospore is nearly spherical. The partial electron-opaque layer (arrows) on the obverse surface of the endospore is unique to this bacterial species. The cortical walls gradually narrow at the base to form a pore unlike that found in *Pasteuria penetrans* or that found in parasites of the cyst nematodes.

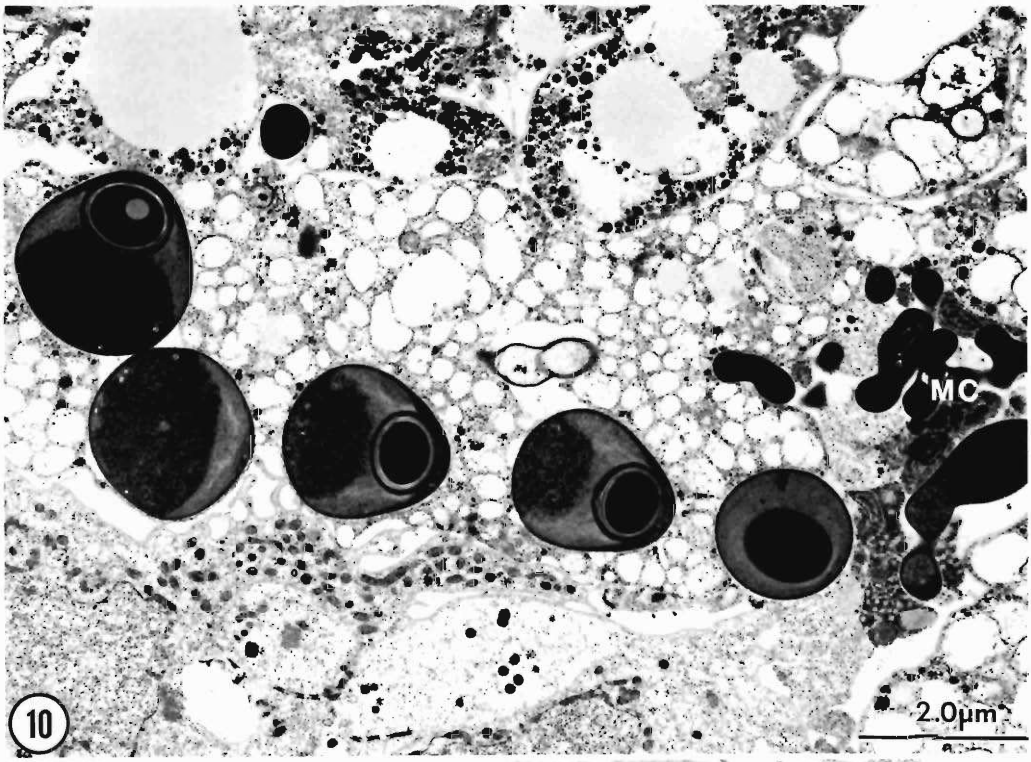

10

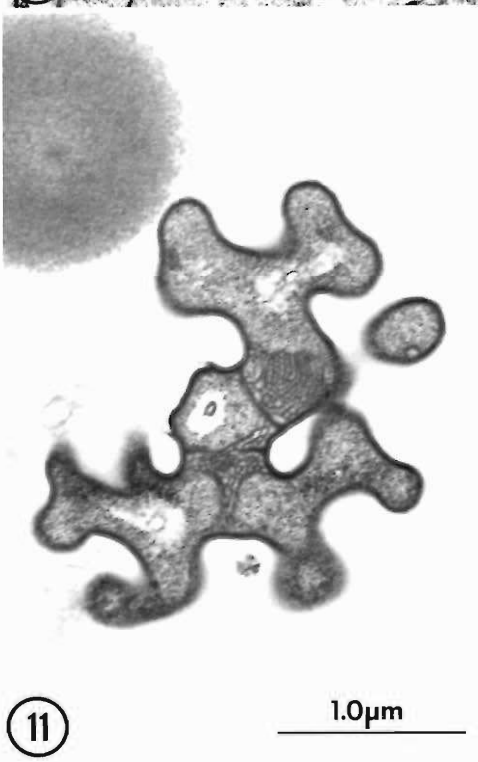

11

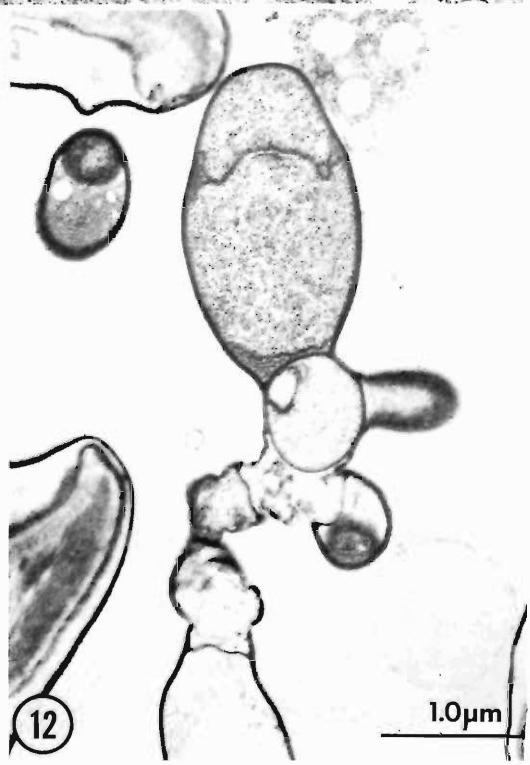

12

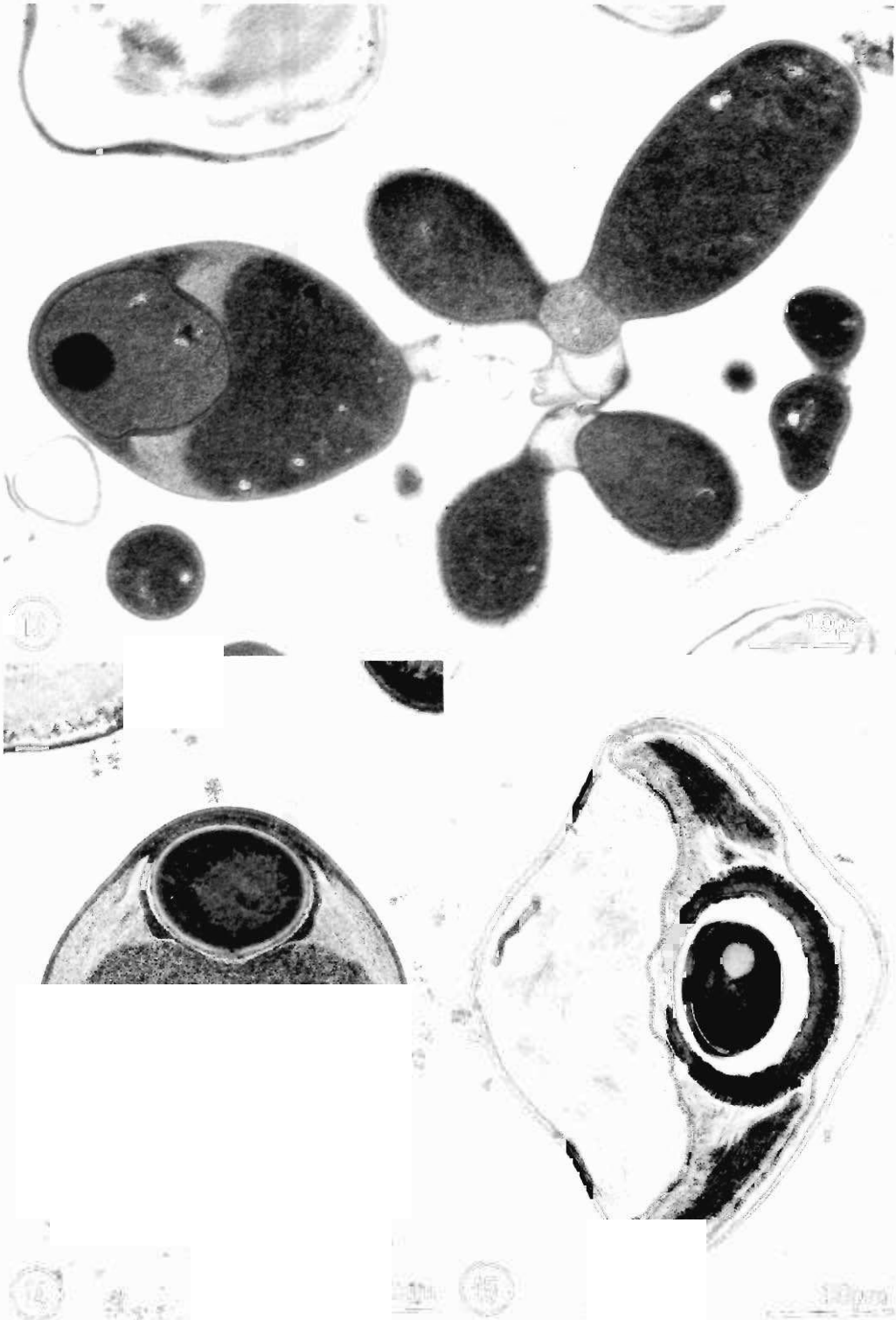

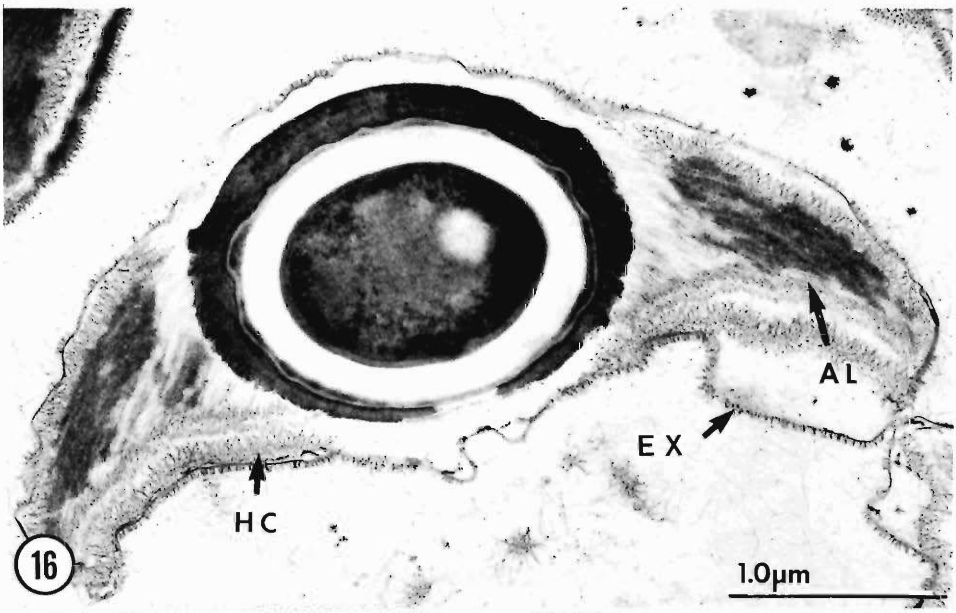

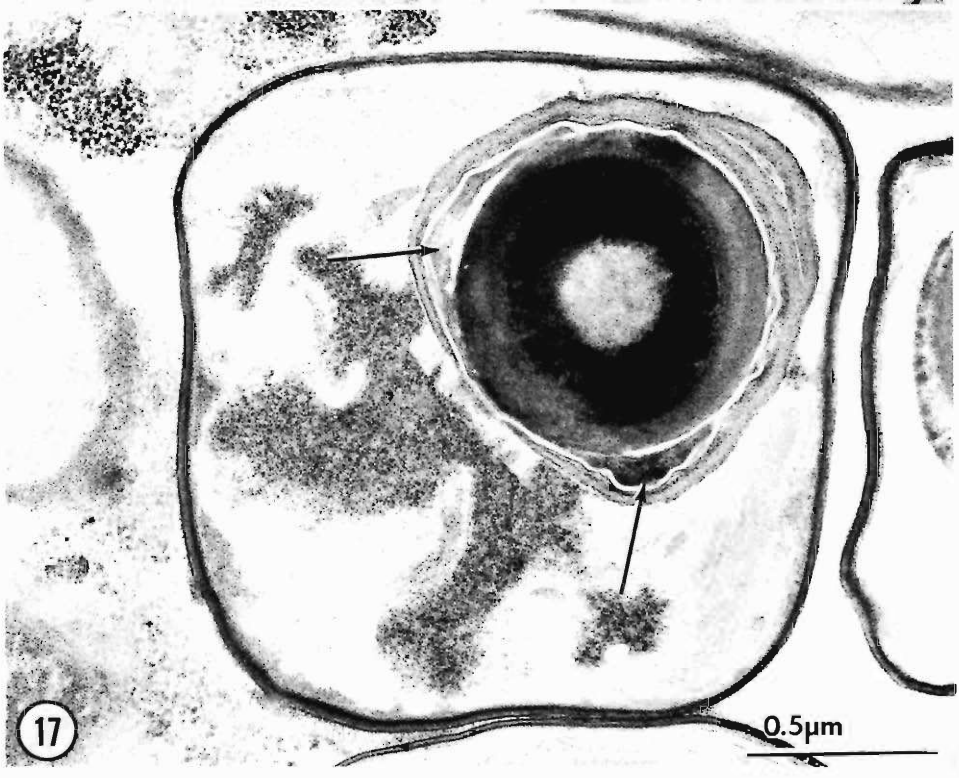

dospores. The outer wall of CNP at the endospore equator measured 0.2 in thickness, and became somewhat thinner toward the base of the central body. A partial layer, hirsute in appearance and originating from the basal adhesion layer of the central body, was unique to CNP (Fig. 16); it has not been observed in members of the genus *Pasteuria.*

Life cycle of CNP

The stages in the life cycle of CNP are similar to those of *P. penetrans* (Table 1). The morphology of all stages of CNP, except the mature sporangium, was similar to that of *P. penetrans.* In addition, the stages in CNP development are in synchrony with those of its cyst nematode host, a relationship that was also found in *P. penetrans.* This synchrony was absent in *P. thornei,* which completed its life cycle in all stages of the host nematode.

CNP also differed from *P. penetrans* in that endospores of the former attached to the adult males of *H. glycines,* but males of *M. incognita* were never observed encumbered by endospores. However, the completion of the life cycle of the bacterium within the males of either nematode species has not been observed.

Host range studies of CNP

In the host range studies of CNP, the attachment of endospores to the respective host J_2 was used as the criterion for susceptibility to the bacterial disease (Fig. 3). The hosts were restricted to species of root-knot and cyst nematodes (Table 2). The endospores of CNP attached to the cyst nematodes but not to root-knot nematodes or to other plant-parasitic or free-living species.

Discussion

Preparatory methods for light microscopic (LM) observations caused least shrinkage to endospores compared to those used in scanning (SEM) and transmission electron microscopy (TEM). Consequently, LM measurements were considered more indicative of the true morphological values. Unfortunately, the small size of the endospore (i.e., 3.5–5.3), and its inherent resistance to staining, limited the LM observations to a few external measurements (Table 1). Nevertheless, these few measurable differences, plus the distinct host range of the bacterial species as expressed by attachment to specific nematode species, were sufficient indicators of isolate differences and helped to delineate and characterize the CNP isolate. Another characteristic that distinguished bacterial isolates at the LM level was their differential abilities to develop in the juvenile stages of nematodes. *Pasteuria thornei* completed its entire life cycle in all stages of the nematode *P. brachyurus* (Sayre et al., 1988). The other species examined could not. Also, the number of sporangia of *P. penetrans* in females of the root-knot nematode was 4 times greater than the number of CNP sporangia in the cyst nematodes. Only a few hundred sporangia were formed in each stage of *P. brachyurus.* These differences are partly due to the smaller volume of vermiform and cyst nematodes compared to that of the swollen root-knot nematode female.

The preparatory methods for SEM caused more shrinkage than those for LM; however, resolution and definition of surface features were far superior with SEM compared to LM. In particular, LVFE SEM revealed details of the external morphology of sporangia and endospores of CNP that had not been resolved in the earlier SEM studies of the other isolates. The episporic wall coverings of *P. penetrans* were found to be relatively smooth, while those of CNP were velutinous to hairy. Additionally, SEM revealed differences in the attachment of episporic wall to the endospore that were not evident in the LM photomicrographs.

In TEM investigations, some fine structural features were common to all species of *Pasteuria* and the CNP (Table 1). Mycelial cell walls of all isolates were typical of the Gram-positive bacteria. During vegetative cell division, mesosomes were often associated with developing septa in all species. The stages of endogenous spore formation, which were typical of Gram-positive rod bacteria, also occurred in all members of *Pasteuria* that have been examined.

Some qualitative differences associated with spore coats of CNP separated this isolate from *P. penetrans* and *P. thornei.* The epicortical spore coat of CNP completely surrounded its central protoplast, but analogous coats were only partially complete in the other 2 species.

Other differences among the endospores of the CNP and *Pasteuria* spp. were the shape and depth of the basal pore. In *P. penetrans,* the wall thickened to form a doughnut-shaped structure that surrounded the pore. In *P. thornei,* the wall tapered to form the opening at the base of the endospore. In CNP, the wall of the endospore neither tapered nor appreciably thickened; thus, the depth of the pore reflected the thickness of

the wall. In addition to this feature, the CNP had a partial wall, which formed on the obverse face of the endospore, that appeared to arise from the endospore attachment layer. These morphologic differences, as revealed by LM, SEM, and TEM, suggest that the CNP isolate is a new species of *Pasteuria.*

Acknowledgments

We are grateful to Drs. D. Sturhan and L. Francl for their critical readings of this manuscript; to Phoebe Betty Starr for skilled bibliographic and redactional assistance; and to C. Pooley, G. H. Kaminski, R. W. Reise, and S. V. Blohm for their proficient technical assistance.

Literature Cited

Ayoub, S. M. 1980. Plant Nematology an Agricultural Training Aid. State of California, Department of Food and Agriculture, Sacramento. 157 pp.

Chapman, R. A. 1957. The effects of aeration and temperature on the emergence of species of *Pratylenchus* from roots. Plant Disease Reporter 41: 836–841.

Huettel, R. N., and R. V. Rebois. 1985. Culturing plant-parasitic nematodes using root explants. Pages 155–158 *in* B. M. Zuckerman, W. F. Mai, and M. B. Harrison, eds. Laboratory Manual for Plant Nematology. Massachusetts Agricultural Experiment Station, Amherst.

Iterson, W. V., ed. 1988. Inner Structures of Bacteria. Van Nostrand Reinhold Co., New York. 302 pp.

Lauritis, J. A., R. V. Rebois, and L. S. Graney. 1982. Technique for gnotobiotic cultivation of *Heterodera glycines* Ichinohe on *Glycine max* (L.) Merr. Journal of Nematology 14:422–424.

———, ———, **and** ———. 1983a. Life cycle of *Heterodera zeae* Kozky, Swarup and Sethi on *Zea mays* L. axenic root explants. Journal of Nematology 15:115–119.

———, ———, **and** ———. 1983b. Development of *Heterodera glycines* Ichinohe on soybean, *Glycine max* (L.) Merr., under gnotobiotic conditions. Journal of Nematology 15:272–281.

Niblack, T. R., and R. S. Huang. 1985. Extracting nematodes from soil and plant tissue, exercise 34. Pages 201–206 *in* B. M. Zuckerman, W. F. Mai, and M. B. Harrison, eds. Laboratory Manual for Plant Nematology. Massachusetts Agricultural Experiment Station, Amherst.

Nishizawa, T. 1984. Effects of two isolates of *Bacillus penetrans* for control of root-knot nematodes and cyst nematodes. Proceedings First International Congress of Nematology. Pp. 60–61.

———. 1986. On an isolate of *Pasteuria penetrans* parasitic to cyst nematodes. Revue de Nematologie 9:303–304.

———. 1987. A decline phenomenon in a population of the upland cyst nematode, *Heterodera elachista,* caused by a bacterial parasite, *Pasteuria penetrans.* Journal of Nematology 19:546.

Sayre, R. M., R. L. Gherna, and W. P. Wergin. 1983. Morphological and taxonomic reevaluation of *Pasteuria ramosa* Metchnikoff 1888 and "*Bacillus penetrans*" Mankau 1975. International Journal of Systematic Bacteriology 33:636–649.

———, **and M. P. Starr.** 1985. *Pasteuria penetrans* (ex Thorne 1940) nom. rev., comb. n., sp. n., a mycelial and endospore-forming bacterium parasitic in plant-parasitic nematodes. Proceedings of the Helminthological Society of Washington 52: 149–165.

———, **and** ———. 1989. Genus *Pasteuria* Metchnikoff 1888, 166^{AL} emend. Sayre and Starr 1985. 149, Starr and Sayre 1988a, 27 (Nom. Cons. Opin. 61 Jud. Comm. 1986, 119. Not *Pasteuria* in the sense of Henrici and Johnson (1935), Hirsch (1972), or Staley (1973); see Starr et al. (1983) and Judicial Commission (1986). Pages 2601–2614 *in* S. T. Williams et al., eds. Bergey's Manual of Systematic Bacteriology. Vol. 4. Williams and Wilkins, Baltimore.

———, ———, **A. M. Golden, W. P. Wergin, and B. Y. Endo.** 1988. Comparison of *Pasteuria penetrans* from *Meloidogyne incognita* with a related mycelial and endospore-forming bacterial parasite from *Pratylenchus brachyurus.* Proceedings of the Helminthological Society of Washington 55:28–49.

———, **and W. P. Wergin.** 1977. Bacterial parasite of a plant nematode: morphology and ultrastructure. Journal of Bacteriology 129:1091–1101.

Southey, J. F., ed. 1986. Laboratory Methods for Work with Plant and Soil Nematodes, 6th ed. [Reference Book 402, Ministry of Agriculture, Fisheries and Food, United Kingdom.] Her Majesty's Stationery Office, London. 202 pp.

Spurr, A. R. 1969. A low viscosity epoxy resin embedding medium for electron microscopy. Journal of Ultrastructural Research 26:31–34.

Starr, M. P., and R. M. Sayre. 1988. *Pasteuria thornei* sp. nov. and *Pasteuria penetrans* sensu stricto emend., mycelial and endospore-forming bacteria parasitic, respectively, on plant-parasitic nematodes of the genera *Pratylenchus* and *Meloidogyne.* Annals de l'Institut Pasteur/Microbiologie 139:11–31.

Stirling, G. R., and M. F. Wachtel. 1980. Mass production of *Bacillus penetrans* for the biological control of root-knot nematodes. Nematologica 26: 308–312.

Sussman, A. S., and H. O. Halvorson. 1966. Spores: Their Dormancy and Germination. Harper and Row, New York. 354 pp.

Wergin, W. P. 1985. Three-dimensional imagery and quantitative analysis in SEM studies of nematodes. Agriculture, Ecosystems, and Environment 12:317–334.

———, **and R. M. Sayre.** 1988. Applications of low voltage field emission SEM in nematology. Journal of Nematology 20:663.

———, ———, **and T. W. Reilly.** 1988. Low-voltage field-emission scanning electron microscopy applications in nematology. Proceedings of the 46th Annual Meeting of the Electron Microscopy Society of America. Pp. 420–421.